

AD-A031 362

AEROSPACE CORP EL SEGUNDO CALIF SPACE SCIENCES LAB
ON THE ROLE OF CHARGE EXCHANGE IN GENERATING UNSTABLE WAVES IN --ETC(U)
OCT 76 J M CORNWALL

F/G 4/1

F04701-76-C-0077

UNCLASSIFIED

TR-0077(2260-20)-1

SAMSO-TR-76-211

NL

| of |
AD
A031362

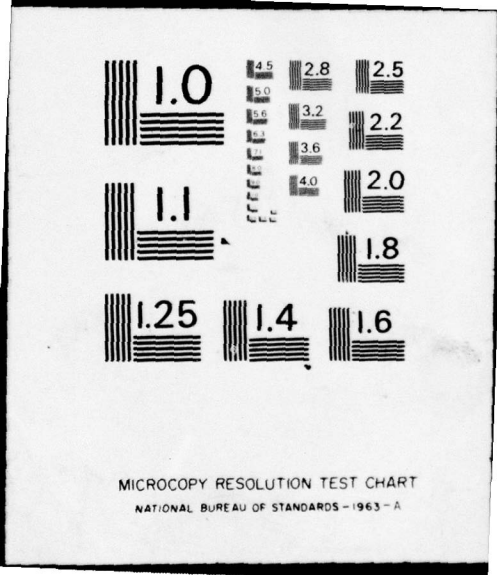


END

DATE

FILMED

11 - 76



MICROCOPY RESOLUTION TEST CHART
NATIONAL BUREAU OF STANDARDS - 1963 - A

REPORT SAMSO-TR-76- 211

AD A031362

12

On the Role of Charge Exchange in Generating Unstable Waves in the Ring Current

Space Sciences Laboratory
Laboratory Operations
The Aerospace Corporation
El Segundo, Calif. 90245

5 October 1976

Interim Report

D D C
RECEIVED
OCT 29 1976
S. J. GILBERT

APPROVED FOR PUBLIC RELEASE;
DISTRIBUTION UNLIMITED

Prepared for
SPACE AND MISSILE SYSTEMS ORGANIZATION
AIR FORCE SYSTEMS COMMAND
Los Angeles Air Force Station
P.O. Box 92960, Worldway Postal Center
Los Angeles, Calif. 90009

This report was submitted by The Aerospace Corporation, El Segundo, CA 90245, under Contract F04701-75-C-0076 with the Space and Missile Systems Organization, Deputy for Advanced Space Programs, P.O. Box 92960, Worldway Postal Center, Los Angeles, CA 90009. It was reviewed and approved for The Aerospace Corporation by G. A. Paulikas, Director, Space Sciences Laboratory. Lieutenant Jean Bogert, SAMSO/YAPT, was the project officer.

This report has been reviewed by the Information Office (IO) and is releasable to the National Technical Information Service (NTIS). At NTIS, it will be available to the general public, including foreign nations.

This technical report has been reviewed and is approved for publication. Publication of this report does not constitute Air Force approval of the report's finding or conclusions. It is published only for the exchange and stimulation of ideas.

AC Form 101-101

NTIS	World Section	<input checked="" type="checkbox"/>
F. G.	Excl. Section	<input type="checkbox"/>
Manuscript		
Justification		
BY	DISTRIBUTION AVAILABILITY CODES	
Dist.	EXCL. and SPECIAL	

A

FOR THE COMMANDER

Jean Bogert
Jean Bogert
1st Lt, United States Air Force
Technology Plans Division
Deputy for Advanced Space Programs

UNCLASSIFIED

SECURITY CLASSIFICATION OF THIS PAGE (When Data Entered)

19 REPORT DOCUMENTATION PAGE		READ INSTRUCTIONS BEFORE COMPLETING FORM
18 REPORT NUMBER SAMS0-TR-76-211	2. GOVT ACCESSION NO.	3. RECIPIENT'S CATALOG NUMBER
6 4. TITLE (and Subtitle) ON THE ROLE OF CHARGE EXCHANGE IN GENERATING UNSTABLE WAVES IN THE RING CURRENT.	5. TYPE OF REPORT & PERIOD COVERED Interim rept.	9
7. AUTHOR(s) John M. Cornwall (Consultant)	10. PROGRAM ELEMENT, PROJECT, TASK AREA & WORK UNIT NUMBERS	14 PERFORMING ORG. REPORT NUMBER TR-0077(2260-20)-1
9. PERFORMING ORGANIZATION NAME AND ADDRESS The Aerospace Corporation El Segundo, Calif. 90245	11. CONTROLLING OFFICE NAME AND ADDRESS Space and Missile Systems Organization Air Force Systems Command Los Angeles, Calif. 90009	15 CONTRACT OR GRANT NUMBER(s) F04701-76-C-0077
14. MONITORING AGENCY NAME & ADDRESS (if different from Controlling Office) 1242p.	12. REPORT DATE 5 October 1976	13. NUMBER OF PAGES 39
16. DISTRIBUTION STATEMENT (of this Report) Approved for public release; distribution unlimited.	15. SECURITY CLASS. (of this report) Unclassified	15a. DECLASSIFICATION/DOWNGRADING SCHEDULE
17. DISTRIBUTION STATEMENT (of the abstract entered in Block 20, if different from Report)	18. SUPPLEMENTARY NOTES	
19. KEY WORDS (Continue on reverse side if necessary and identify by block number) Ring Current Wave Particle Interactions Charge Exchange	20. ABSTRACT (Continue on reverse side if necessary and identify by block number) We explore the role of charge exchange in generating anisotropy in the ring current during recovery phase inside the plasmopause. A simplified scenario is studied, in which the anisotropy evolves from an initially isotropic distribution. Other cases may be easily studied by shifting the time axis. When the anisotropy becomes large enough, the proton ring current just inside the plasmopause will emit ion electromagnetic cyclotron waves (which can cause SAR arcs by electron heating), with subsequent destruction of anisotropy in ^{is explored,} (continued) → next page	

DD FORM 1473 (FACSIMILE)

UNCLASSIFIED

SECURITY CLASSIFICATION OF THIS PAGE (When Data Entered)

407512 AB

UNCLASSIFIED

SECURITY CLASSIFICATION OF THIS PAGE (When Data Entered)

19. KEY WORDS (Continued)

20. ABSTRACT (Continued)

cont. → the wave-emission process. As long as finite-amplitude waves are present, gain and loss of anisotropy will be in rough equilibrium, and the pitch-angle distribution will no longer evolve as it would if only charge exchange were operating. The amount of energy lost to the waves is related to the charge-exchange loss rate with the aid of quasi-linear moment equations; it seems to be adequate to power SAR arcs. The role of heavy ions (He^+ , He^{++} , O^+) is considered; generally, these ions tend to damp the proton-generated waves. This damping is quite sensitive to the very-low-energy ($<1 \text{ keV}$) portion of the heavy-ion distribution function, but not to the thermal ($\sim \text{eV}$) component. If the heavy-ion fraction at beginning of recovery phase is ≤ 0.2 , proton EMC waves will most likely not be generated by charge exchange beginning from initial isotropy.

less than or equal to

UNCLASSIFIED

CONTENTS

I.	INTRODUCTION	3
II.	GROWTH RATES AS DETERMINED BY CHARGE EXCHANGE ..	7
III.	COUPLED CHARGE-EXCHANGE AND ION-EMC EMISSION EFFECTS	21
IV.	DYNAMICS ACCORDING TO THE MOMENT TRANSPORT EQUATIONS	29
	APPENDIX	37
	REFERENCES	39

FIGURES

1.	Proton charge exchange rate λ_o , for equatorially mirroring particles.	8
2.	Growth rate divided by group velocity (unnormalized), for case I ($N = \text{constant}$), $E_m/E_o = 0.21$	13
3.	Growth rate divided by group velocity and time (unnormalized), for case II (N proportional to t), $\lambda_o t E_m/E_o = 0.21$	15
4.	Pitch-angle shape parameter τ vs. anisotropy A	24
5.	Pitch-angle averaged charge-exchange rate Λ vs. anisotropy A	26
6.	Dependence of the maximum growth rate Γ_{MAX} on anisotropy A	28

I. INTRODUCTION

In spite of many years of theoretical and experimental effort, there is still no convincing picture of ring current dynamics during geomagnetic storms. Even such mundane processes as charge exchange do not seem to play a simple, clear role. For example, the apparent agreement between observed ring-current decay and calculated charge-exchange lifetimes [Liemohn, 1961] as found by Swisher and Frank [1968] and Smith et al. [1975] has been challenged by Tinsley [1976] and by Lyons and Evans [1976], partly on the grounds that Liemohn's lifetimes are too long (in view of recent results on neutral hydrogen density) and partly on the grounds that pitch-angle distributions of low-energy ions do not behave in agreement with calculation. These authors conclude that, after a few hours of recovery phase, a large fraction of the ring current is He^+ (which for $E < 50$ keV has a longer charge-exchange lifetime than a proton of the same energy). The picture is further complicated by the discovery of energetic precipitating O^+ ions apparently associated with the storm-time ring current [Shelley et al., 1974] which also have a long charge-exchange lifetime.

Charge exchange is an important source of anisotropy for ring-current protons. When this anisotropy becomes large enough, it leads to the generation of ion electromagnetic cyclotron (EMC) waves [Cornwall et al., 1970] which can cause further proton losses and possibly make SAR arcs by heating electrons [Cornwall et al., 1971]. In this paper we explore the interplay between the charge-exchange process, the rate at which energy and anisotropy is lost during the wave-emission process, and the influence of heavy ions on wave emission and absorption. Four major features emerge:

(1) With the aid of simplifying (but realistic) assumptions, a convenient analytic expression for the wave growth rate as a function of time, of the

parameters of the distribution function, and of the cold plasma density is found, for the case of an initially isotropic distribution. During recovery phase, as the cold plasma density increases, the maximum growth rate occurs at a ratio of frequency ω to proton gyrofrequency Ω of $\omega/\Omega \approx 0.4$, independent of time.

(2) The proton anisotropy A grows (while the flux decays) to the point where finite-amplitude ion-EMC waves are emitted, if the initial flux is large enough. For some time thereafter, A is roughly constant, because there is near-balance between charge-exchange growth of A and decrease of A by wave emission. During this phase, the anisotropy is roughly governed by the well-known expression

$$E_R = \frac{B^2}{8\pi N} \frac{1}{A^2(1+A)} \quad (1.1)$$

where E_R is the resonant parallel proton energy, B the earth's field, and N the total plasma density. Relation (1.1) is fairly well satisfied experimentally [Williams and Lyons, 1974a]. The fact that the anisotropy ceases to evolve after a certain time is an important consideration for comparing observations with theory. Eventually A begins to grow again, in order to keep up the wave growth rate in the face of a decaying flux of ring-current protons.

(3) The rate at which protons lose energy to the waves is governed by the charge-exchange loss rate, when the only source of anisotropy is charge exchange. At first sight this may seem somewhat surprising, in view of the gross discrepancy between charge-exchange time scales and wave-growth time scales. The simplest statement [Cornwall, 1975b] of this effect follows from the single-particle emission picture put forward by Brice [1964]. A more

realistic treatment is based on the quasi-linear moment equations of Cornwall [1975a]. We show that sufficient energy is generated to power SAR arcs.

(4) If heavy ions (He^+ , He^{++} , O^+) are initially isotropic, charge exchange will do little to change this during the first few proton lifetimes (except for He^{++} above ~ 10 keV). Consequently, these ions act to damp the proton-EMC waves; a heavy-ion fraction of 0.2 at beginning of recovery phase is enough to prevent wave growth altogether. This damping is quite sensitive to the very-low-energy (< 1 keV) part of the heavy-ion distribution function, which remains unmeasured. In this paper, we do not consider time scales so long that heavy ions have acquired large anisotropies by charge exchange.

A clear idea of the role of charge exchange in ring-current dynamics can only be gotten at the expense of ignoring other potentially important effects. For example, there are most likely additional sources of both proton flux and anisotropy (e.g., radial diffusion), and there is experimental evidence [Williams and Lyons, 1974a,b] that the plasmopause is a boundary inside or outside of which certain effects do not act. This evidence is that the pitch-angle distributions for $E < 50$ keV protons outside the plasmopause do not evolve into the sort of anisotropic distributions seen inside; rather, they become isotropic except for the loss cone (flat-topped). This could be because of an additional source (convection) or relatively weak pitch-angle diffusion mechanism, such as an electrostatic instability, which acts only outside the plasmopause. Or it could be, as Joselyn and Lyons [1976] point out, that $E < 50$ keV protons pick up their anisotropy as they are irradiated by ion-EMC waves generated off the equator by higher-energy protons, which are continually anisotropic. (We note that the required cyclotron-resonant energy of the higher-energy off-equatorial protons varies rather steeply with distance from the equator, roughly like $\sin^{-2}\theta$, where θ is the colatitude.) The fact

that we do not consider such effects here does not mean that we consider them unimportant; we omit them only for the sake of clarity.

Finally there are the questions of what the initial anisotropy of the low-energy ($E \lesssim 50$ keV) ring current is, at the beginning of recovery phase, and whether these initial distributions evolve consistent with charge exchange losses. The general impression from the S^3 data for the December 17-18, 1971 storm [Williams and Lyons, 1974a, b] is that it is reasonably isotropic inside the plasmasphere (although not really flat) and that the anisotropy grows some during recovery phase, except at energies below ≈ 10 keV. (This latter effect has motivated Tinsley [1976] and Lyons and Evans [1976] to suggest that this part of the ring amount is largely He^+ .) However, there is by no means quantitative evidence that the ring current 10-50 keV evolves consistent with an initially flat distribution, with charge exchange as the only major effect, or that the total flux decay rate of the December 17-18 storm is consistent with charge exchange. We persist with our idealized scenario of initially flat pitch-angle distributions evolving according to charge exchange because: (a) To some extent, the effect of pre-existing anisotropies at the beginning of recovery phase can be modeled by shifting the time axis and renormalizing the growth rates; (b) it is important to know something about the theory of the mutual influence of charge exchange and wave emission on the pitch-angle distributions; and (c) whatever other effects act on the ring current, charge exchange is always there.

II. GROWTH RATES AS DETERMINED BY CHARGE EXCHANGE

A. Contributions from Protons

Because the magnetospheric hydrogen density is greatest at low altitudes, the charge-exchange loss rate $\lambda(E,L,\alpha)$ is a function of equatorial pitch angle α , or of $y = \sin\alpha$. It is reasonably well-fit by a power law:

$$\lambda = \lambda_0(E,L) y^{-n} \quad (2.1)$$

Liemohn [1961] first calculated λ for magnetospheric applications, and found $n \approx 2$. We agree with Tinsley [1976] that Liemohn's values of λ are too small, because he used too small a value for the neutral hydrogen density. In fact, orbit-averaged neutral hydrogen densities calculated some time ago [Cornwall et al., 1965] are reasonably close to Tinsley's values, and larger than Liemohn's. The proton charge-exchange rates based on Cornwall et al. are shown in Fig. 1. A fit to Eq. (2.1) gives a value of n somewhat less than 2 (as already noted by Cornwall [1975a]), but throughout this paper we use $n = 2$ because it results in simple analytic expressions for the ion-EMC growth rate. Note that from Fig. 1 the time scale λ_0^{-1} for protons has a minimum value of ~ 4 hours at $L = 3$, $E \approx 3-15$ keV. The time scale is even less off the equator.

At $t = 0$ (beginning of recovery phase) we assume, in accordance with the scenario of Section I, that the protons of $E \lesssim 50$ keV near the plasmasphere (which has shrunk to $L \approx 3$) have an isotropic distribution function. An eyeball fit to smoothed-out data of Williams and Lyons is roughly exponential with an e-folding energy E_0 of ~ 15 keV at $L = 3$. The differential flux J evolves in time as

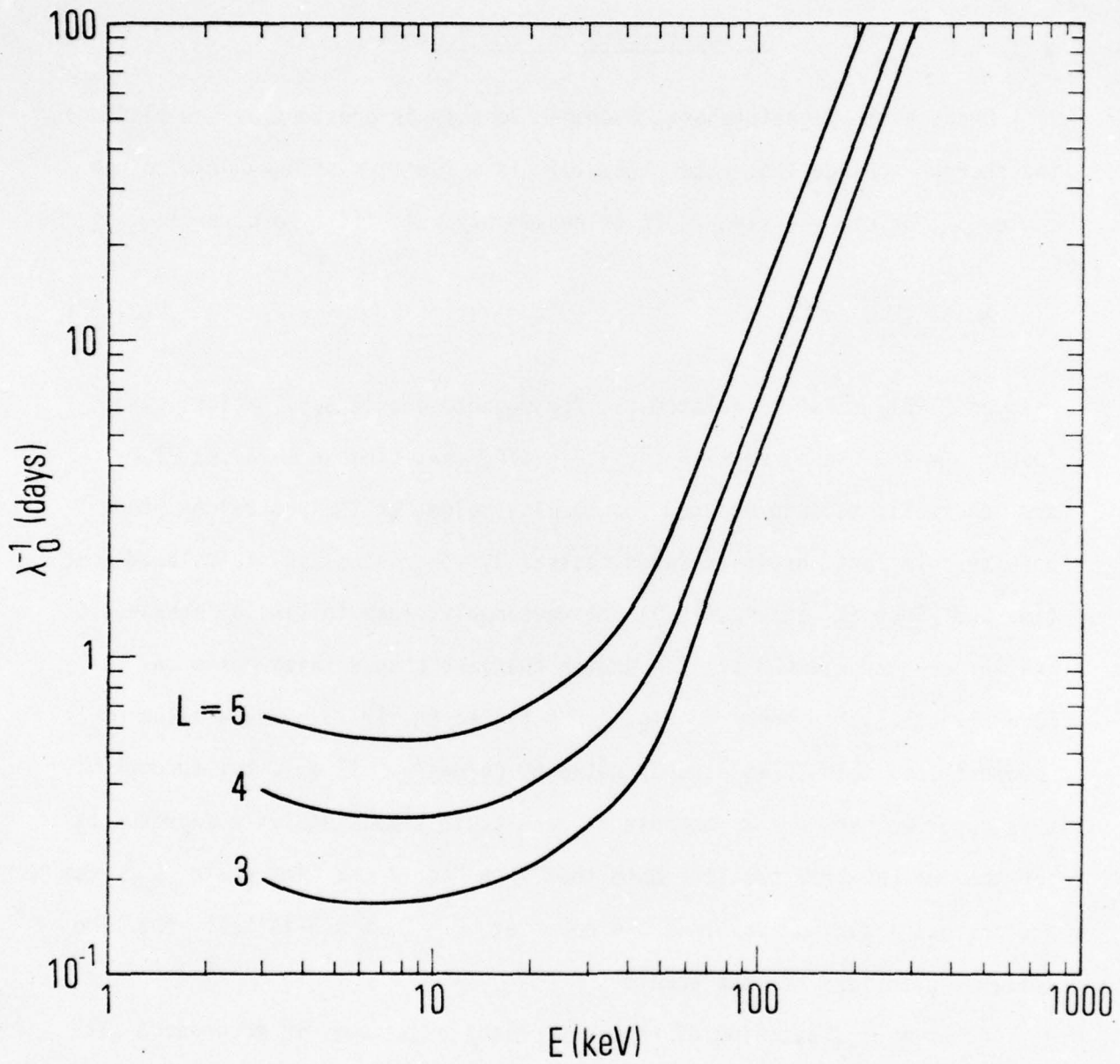


Figure 1. Proton charge exchange rate λ_0 , for equatorially mirroring particles.

$$J(E, y, L, t) = J_0(E, L) \exp\{-\lambda_0(E, L) t y^{-2}\} \quad (2.2)$$

$$J_0(E, L) = J_0(L) e^{-E/E_0} \quad (2.3)$$

Let us calculate the growth rate γ of proton-EMC waves, normalized to the convective loss rate $v_G/2\ell$, where v_G is the group velocity and ℓ a length characteristic of the field line:

$$\begin{aligned} \frac{2\gamma\ell}{v_G} &= \left(\frac{2\ell}{v_G} \right) \frac{4\pi^3}{|k|} \left(\frac{e}{Mc} \right)^2 v_G v_p \\ &\times \int dE dy \delta(y-y_0) \left[-f + \frac{1}{2} \left(\frac{\Omega}{\omega} - 1 \right) y \frac{\partial f}{\partial y} \right]. \end{aligned} \quad (2.4)$$

Here v_p is the phase velocity, M the proton mass, and

$$y_0 = \left[1 - \left(\frac{\Omega - \omega}{kv} \right)^2 \right]^{1/2} = \left[1 - \frac{E_m}{E} \frac{(1-x)^3}{x^2} \right]^{1/2} \quad (2.5)$$

with $E_m = B^2/8\pi N$ as the magnetic energy per particle. The distribution function f is related to J by $f = M^2(2E)^{-1}J$. Using this, (2.2) and (2.3) in (2.4) yields

$$\begin{aligned} \frac{2\gamma\ell}{v_G} &= \frac{\pi^2 \ell M \Omega}{N} \left(\frac{1-x}{x} \right) \int_{E_c} \frac{dE}{E} J_0(L) \left[-1 + \left(\frac{1-x}{xy_0^2} \right) \lambda_0 t \right] \\ &\times \exp\{-E/E_0 - y_0^{-2} \lambda_0 t\} \end{aligned} \quad (2.6)$$

where $E_c = E_m(1-x)^3 x^{-2}$, $y_0^2 = 1 - (E_c/E)$.

As t increases, the anisotropy factor (in square brackets) increases, while the current decreases exponentially. Therefore $2\gamma\ell v_G^{-1}$ has a maximum; for finite-amplitude ion-EMC waves to occur, this maximum must be greater

than unity. The integral in (2.6) is manageable if we approximate λ_0 by a constant independent of E (but depending on L); Fig. 1 shows that this is reasonable for $E \leq 30$ keV. We then find, as shown in the Appendix,

$$\frac{2\gamma\ell}{v_G} = \frac{J_0(L) \pi^2 \ell M \Omega}{N} \left(\frac{1-x}{x} \right) \exp\{-\lambda_0 t - E_c/E_0\} \left[2\lambda_0 t \left(\frac{1-x}{x} \right) K_0(z) - Q(a,z) \right] \quad (2.7)$$

$$z = 2 \left(\frac{\lambda_0 t E_c}{E_0} \right)^{1/2}, \quad a = \left(\frac{E_c}{\lambda_0 t E_0} \right)^{1/2} = \frac{z}{2\lambda_0 t} \quad (2.8)$$

$K_0(z)$ is a Hankel function of imaginary argument. The closely-related function Q is non-standard, but easy to handle. It is described in detail in the Appendix, where it is shown that

$$Q(a,z) + Q(a^{-1},z) = 2K_0(z) \quad (2.9)$$

$$Q(0,z) = 2K_0(z); \quad Q(1,z) = K_0(z) \quad (2.10)$$

Furthermore, Q is a positive decreasing function of a for $0 \leq a \leq \infty$, all z , thus bounded by 0 and $2K_0(z)$. A simple approximation to $Q(a,z)$ which satisfies (2.9) and (2.10) is

$$Q(a,z) \approx \frac{2K_0(z)}{1+a} \quad (2.11)$$

Although strictly speaking the derivation of (2.11) is only valid for large z , (2.11) can be used with acceptable accuracy (~15%) down to $z \approx 0.1$, and is accurate to $\leq 3\%$ for $z \sim 1$. Substitute (2.11) into (2.7) to find the normalized growth rate

$$\frac{2\gamma\ell}{v_G} \approx \frac{2\pi^2 J_0(L) M\Omega\ell}{N} \left(\frac{1-x}{x} \right) K_0(z) \left[\lambda_0 t \left(\frac{1-x}{x} \right) - \frac{1}{1+a} \right] \exp\{-\lambda_0 t - E_c/E_0\} . \quad (2.12)$$

The first term in square brackets, proportional to t , represents the buildup of anisotropy from charge exchange. The term $\exp(-\lambda_0 t)$ shows the decay of the total flux. The interaction of the two terms lends to a growth rate γ which builds up and then decays.

It seems natural, by comparison with the growth-rate formula for a bi-Maxwellian or for a distribution function of the form $y^{2A} f(E)$, to identify the anisotropy from (2.12) as

$$A_{\text{eff}} = \lambda_0 t(1+a) = \lambda_0 t + \frac{1}{2} z . \quad (2.13)$$

However, (2.13) is both frequency-dependent and dependent on E_m/E_0 . In Section III, we use another definition of the anisotropy A , which is adapted to the quasi-linear moment equations [Cornwall, 1975a], and which is independent of x and E_m/E_0 . One may remove the frequency dependence in (2.13) by evaluating the right-hand side at the frequency \bar{x} at which the growth rate is maximum; the corresponding \bar{A}_{eff} depends only slightly on E_m/E_0 . (This is because \bar{x} is not far removed from that value of x which makes $E_c \approx E_0$; by the definition (2.8) of z , it follows that \bar{A}_{eff} depends mostly on $\lambda_0 t$). \bar{A}_{eff} does not quite agree with A as defined in Section III, but the maximum difference is < 0.18 over the physically interesting range of variation of other parameters. The reasonable agreement of these two definitions is a signal that the quasi-linear moment equations more or less fairly represent the physics of a ring current decaying by charge exchange and emitting ion-EMC waves.

We now distinguish two different physical circumstances under which (2.12) might be used: (1) N is constant in time; (2) N increases with time. Case (1) is appropriate to protons well inside the plasmapause, while case (2) is appropriate to protons just inside or outside the plasmasphere, as it refills and expands during recovery phase. For simplicity we suppose that N grows linearly with t , from an initial value of zero:

$$N = \dot{N}t, \quad \dot{N} = \text{const.} \quad (2.14)$$

Observe that, from (2.8) and the expression for E_c , z is constant in time (at fixed x) for case (2), and a decreases like t^{-1} .

In Fig. 2, we plot the expression

$$\tilde{\gamma} = \frac{(1-x)}{x} K_0(z) \left[\lambda_0 t \left(\frac{1-x}{x} \right) - \frac{1}{1+a} \right] \exp\{-\lambda_0 t - E_c/E_0\} \quad (2.15)$$

for the special case $E_m/E_0 = 0.21$ (e.g. $L = 3$, $E_0 = 15$ keV, $N = 10^3$).

The normalized growth rate $2\gamma\ell v_G^{-1}$ is, by (2.12),

$$\frac{2\gamma\ell}{v_G} = \frac{2\pi^2 \ell m \Omega}{N} J_0(L) \tilde{\gamma} \quad (2.16)$$

$$\approx 4 \left(\frac{3}{L} \right)^2 \left(\frac{10^3}{N} \right) (J_0(L) \times 10^{-6}) \tilde{\gamma} \quad (2.17)$$

where N is in units of cm^{-3} , $J_0(L)$ in units of $(\text{keV cm}^2 \text{ sec ster})^{-1}$, and $\ell = LR_e$, with $R_e =$ one earth radius. According to Williams and Lyons' data, $J_0(L)$ is typically in the range 10^6 - 10^7 . Fig. 2 is useful for calculating the growth rate in case (1).

In Fig. 3, we plot the expression $\tilde{\gamma}(\lambda_0 t)^{-1}$, useful for calculating the growth rate in case (2), for the special case $\lambda_0 t E_m/E_0 = 0.21$ (e.g.

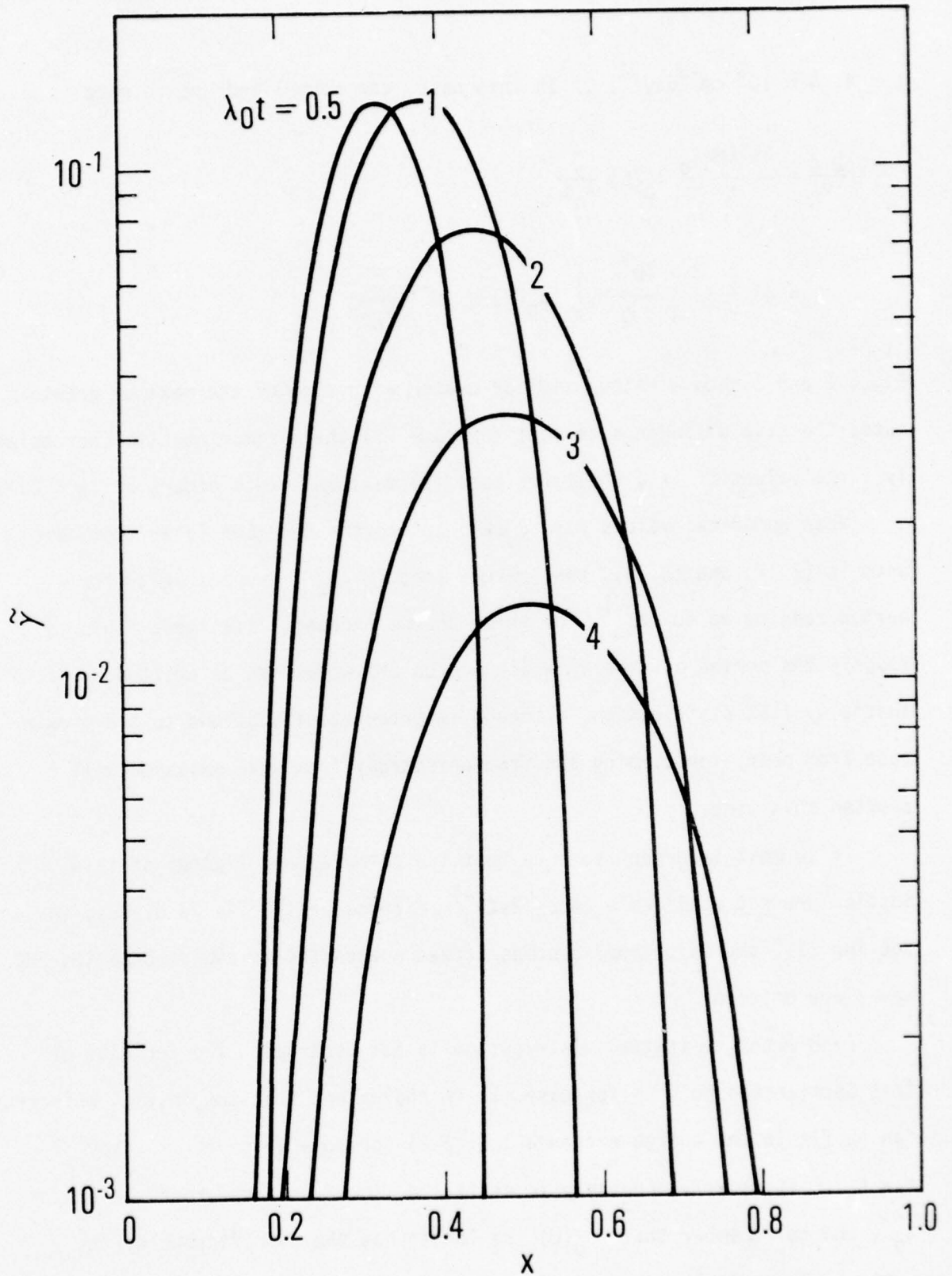


Figure 2. Growth rate divided by group velocity (unnormalized), for case I ($N = \text{constant}$), $E_m/E_0 = 0.21$. To normalize, see Eq. (2.17).

$L = 4, \dot{N} = 10^3 \text{ cm}^{-3} \text{ day}^{-1}$. In this case, the normalized growth rate is

$$\frac{2\gamma\ell}{v_G} = \frac{2\pi^2 \ell_{EM} \lambda_0}{\dot{N}} J_0(L) \frac{\tilde{\gamma}}{\lambda_0 t} \quad (2.18)$$

$$\approx 4 \left(\frac{3}{L} \right)^2 \left(\frac{10^3 \lambda_0}{\dot{N}} \right) (J_0(L) \times 10^{-6}) \frac{\tilde{\gamma}}{\lambda_0 t} \quad (2.19)$$

Figs. 2 and 3 show a rather similar change with time of the maximum growth rate; the main difference is that for case (1) the maximum goes to increasingly large values of x , while for case (2) maximum growth occurs at $x \approx 0.35$.

When numerical values for $J_0(L)$ fit to the December 17-18 storm are used in (2.17) and (2.19), they reveal that $2\gamma\ell v_G^{-1}$ exceeds unity for a period ranging up to $3\lambda_0^{-1}$, or three charge exchange lifetimes. This is roughly the period of time in which proton EMC waves can be emitted by an initially flat distribution, although important modifications to the growth rate from heavy-ion damping and from anisotropy from wave emission will shorten this time.

It is most important to note that the formulas and figures of this Section are not applicable once $2\gamma\ell v_G^{-1}$ exceeds unity. As we discuss in Section III, the anisotropy becomes locked and ceases to evolve once ion-EMC waves are emitted.

Even when the initial distribution is not isotropic, the formulas of this Section can be used for case (1) to the extent that the initial anisotropy can be fit to the charge exchange law (2.2) for some value of t , say $t = t_0$. It is only necessary to shift the time axis backward by an amount t_0 , and to remember that $J_0(L)$ no longer has the significance of the initial perpendicular flux at the equator. In case (2), it is necessary also

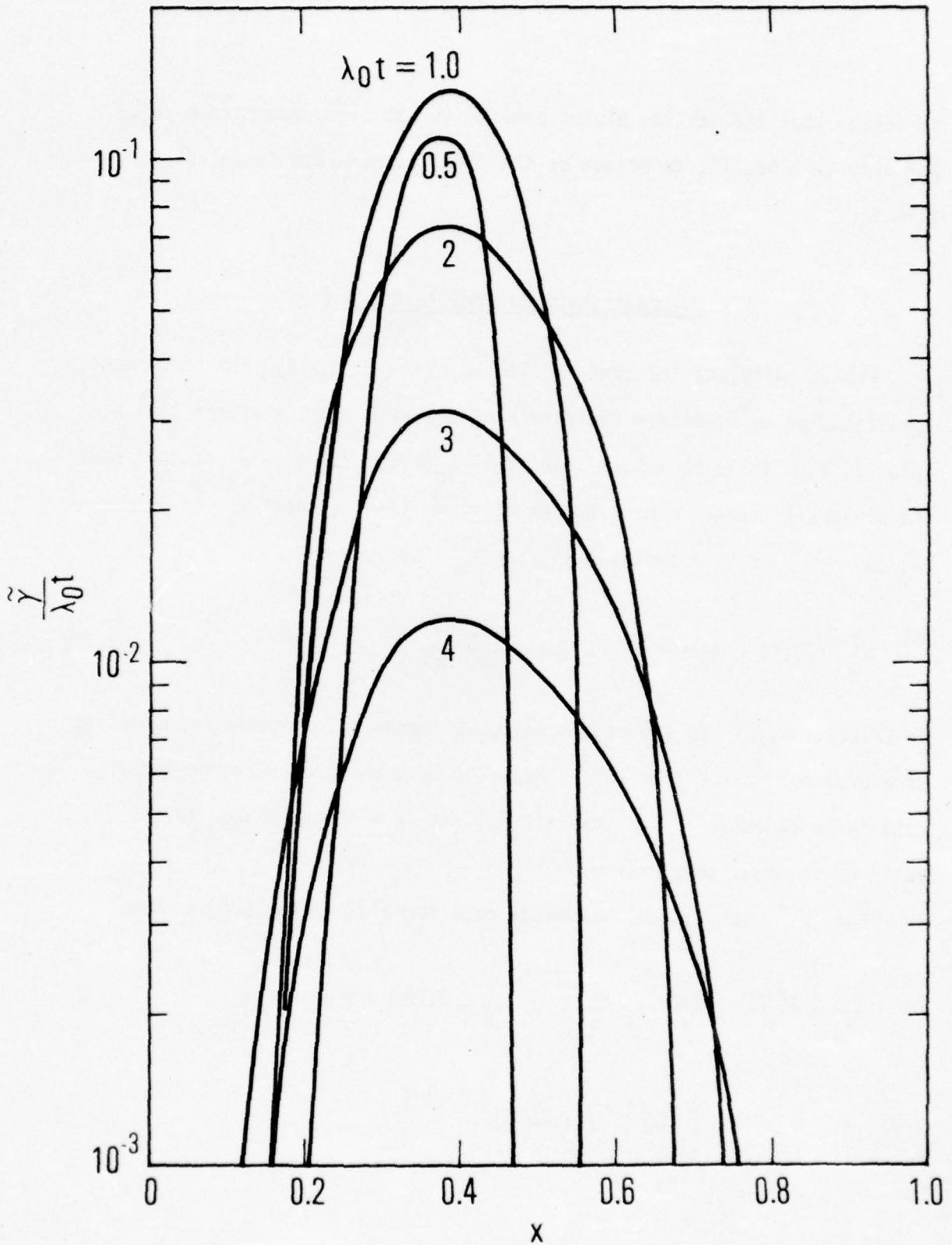


Figure 3. Growth rate divided by group velocity and time (unnormalized), for case II (N proportional to t), $\lambda_0 t E_m/E_0 = 0.21$. To normalize, see Eq. (2.19).

to assume that the initial plasma density is not zero, but rather $\dot{N}_0 t_0$. Normally this has little effect on the final growth-rate formulas, for $t \gg t_0$.

B. Contributions from Heavy Ions

Let us calculate the contribution to $2\gamma_L v_G^{-1}$ coming from heavy ions, specifically He^+ , within the spirit of the same approximations that went into (2.12). It is no longer true that $\lambda_0(L, E)$ is roughly constant over the low-energy range; a much better approximation is that λ_0 is linear in energy. For He^+ , a suitable fit to λ_0 is:

$$\lambda_0^{(\text{He})}(L, E) = \lambda_0'(L)E ; \quad \lambda_0'(L) \approx \frac{\lambda_0(L)}{250 \text{ keV}} . \quad (2.20)$$

In (2.20), $\lambda_0(L)$ is the proton charge-exchange rate, assumed independent of energy for $3 < E < 30$ keV. Above 30 keV, the proton charge-exchange rate falls sharply, and $\lambda_0(\text{He}) \approx \lambda_0(\text{p})$ at $E \approx 50$ keV. Eq. (2.20) is valid up to about this energy.

For He^+ ions, the fundamental rate formulas (2.4)-(2.6) become

$$\frac{2\gamma_L}{v_G} = \frac{\pi^2 \ell M \Omega}{N} \left(\frac{1-x}{x} \right) \int \frac{dE}{E} \left[-J + \frac{1}{2} \left(\frac{\Omega(\text{He})}{\omega} - 1 \right) y \frac{\partial J}{\partial y} \right]_{y=y_0'} \quad (2.21)$$

$$y_0' = \left\{ 1 - \frac{E_m}{E} \left(\frac{1-x}{x^2} \right) \left(x - \frac{\Omega(\text{He})}{\Omega} \right)^2 \right\}^{1/2} \quad (2.22)$$

$$= (1 - E_c'/E)^{1/2}$$

$$E_c' = E_m \left(\frac{1-x}{x^2} \right) \left(x - \frac{\Omega(\text{He})}{\Omega} \right)^2 \quad (2.23)$$

where, as before, $x = \omega/\Omega$, M the proton mass, and Ω is the proton gyrofrequency. We assume that the helium ions are not present in sufficient numbers to modify the phase or group velocity appreciably.

Note that for $x \approx 1/4$, E'_c is much smaller than the corresponding value E_c for protons. For $x \approx 0.35$, the frequency of maximum growth as shown in Fig. 3, $E'_c/E_c \approx 0.02$. Since the integral over E in (2.21) runs down to E'_c , the He^+ distribution function ($\sim J/E$) is probed at very low energies, hundreds of eV or less. This is also so if the ions are He^{++} , but the corresponding ratio E'_c/E_c for O^+ is not as small by nearly an order of magnitude. Even with a positive anisotropy, heavy ions yield a negative contribution to γ as long as $\omega > \Omega(\text{ion})$. A positive heavy-ion contribution to γ is possible for $\omega < \Omega(\text{ion})$, if the heavy-ion anisotropy is large enough. For He^+ , charge exchange probably does not contribute dominantly to this anisotropy, since a typical He^+ charge-exchange time scale is ~ 60 hours at the equator at $L = 3$. (It is about one day for O^+ at the same place.)

If we were to calculate the heavy-ion contribution to γ using $J_0^{(\text{ion})}(E, L) = J'_0(L) e^{-E/E'_0}$, and (2.20) for $\lambda_0(\text{ion})$, a formula similar to (2.12) would emerge. However, this formula would be logarithmically singular at $E'_c = 0$, reflecting the E^{-1} singularity in the heavy-ion distribution function $f \sim J/E$. This is no problem for protons, where E_c can never become too small, but the singularity in f must be removed for the heavy ions. Let us (in the absence of very-low-energy measurements) assume the He^+ current J' to be, at $t = 0$:

$$J'(L, E, t=0) = J'_0(L) \frac{E}{E'_0} e^{-E/E'_0}. \quad (2.24)$$

This Maxwellian phase-space distribution function may be used either for the thermal component or for the ring-current component (in which case presumably $E'_0 \approx E_0$). In analogy with the calculation of (2.12), we find, using (2.20)-(2.24)

$$\begin{aligned} \frac{2\gamma\ell}{v_G} \Big|_{\text{He}^+} &= \frac{\pi^2 \ell M \Omega}{N} \left(\frac{1-x}{x} \right) J'_0(L) \exp(-\bar{\lambda}t - E'_c/E'_1) \left(\frac{z'E'_1}{E'_0} \right) \\ &\times \left\{ -K_1(z') + \left(\frac{0.25-x}{x} \right) \left[\frac{\bar{\lambda}t}{a'} K_2(z') + \bar{\lambda}t K_1(z') + \frac{z'}{2} K_0(z') \right] \right\} \end{aligned} \quad (2.25)$$

where the $K_i(z)$ are Hankel functions of imaginary argument. In (2.25), the following parameters appear:

$$\begin{aligned} \bar{\lambda} &= \lambda'_0 E'_c, \quad z' = 2 \left(\frac{\bar{\lambda}t E'_c}{E'_1} \right)^{1/2}, \quad a' = \frac{z'}{2\bar{\lambda}t}, \\ E'_1 &= E'_0 \left[1 + \bar{\lambda}t \left(\frac{E'_0}{E'_c} \right) \right]^{-1}. \end{aligned} \quad (2.26)$$

This expression is well-behaved at $E'_c = 0$; it is worth noting that the heavy-ion contribution to the growth rate does not decrease exponentially at $E'_c = 0$.

First, consider the contribution of ring-current ($> \text{keV}$) He^+ ions. For all practical purposes, we may set $E'_c = 0$ in (2.25), and ignore the terms in square brackets; this approximation breaks down only after many proton charge-exchange lifetimes or for very small x . Then we find

$$\frac{2\gamma\ell}{v_G} \Big|_{\text{He}^+} \approx \frac{-\pi^2 \ell M \Omega}{N} \left(\frac{1-x}{x} \right) \left[1 + \lambda'_0 t E'_0 \right]^{-1} J'_0(L). \quad (2.27)$$

Then let us take $E'_0 \approx E_0 \approx 15$ keV . The term in square brackets is nearly equal to unity for many proton lifetimes. Finally, let us take the He^+ flux at $E \approx E_0$ and at $t = 0$ to be constant fraction of the proton flux for all L , that is, $J'_0(L) = \zeta J_0(L)$. A very simple modification to the growth-rate formula (2.15) emerges: simply subtract $\frac{1}{2} \zeta \left(\frac{1-x}{x} \right)$ from the right-hand side of this expression for $\tilde{\gamma}$. This may be done directly on Figs. 2, 3. Since ζ might range from 0.05 to 0.2, this can be a very significant negative contribution to the growth rate. In fact, if $\zeta \geq 0.2$, $2\gamma\lambda v_G^{-1}$ will never exceed unity, and proton EMC waves will not be generated.

For O^+ , the charge-exchange rate is also rather small, about an order of magnitude less than that for protons. We may roughly incorporate the effect of O^+ ions by taking ζ to be the ratio $(\text{He}^+ + \text{O}^+)/p$.

For He^{++} , the situation is somewhat different. Between 10 and 30 keV, the charge-exchange rate for $\text{He}^{++} \rightarrow \text{He}^+$ is comparable to the proton charge-exchange rate. The He^{++} contribution is, crudely speaking, given by (2.12) except that inside the square brackets $1-x$ is replaced by $0.5-x$, and E_c is found from (2.23) using $\Omega(\text{He}^{++})/\Omega = 0.5$; the values of a, z from (2.8) are correspondingly modified. In contrast to He^+ , the He^{++}/p ratio (at least from 10 to 30 keV) is roughly constant in time. With $\zeta(\text{He}^{++}) \sim 0.05$ to 0.2 , these ions contribute modestly to growth for $x \approx 0.35$, when $\lambda_0 t \geq 2$, but their main effect is to build up the He^+ population. This can be accounted for by letting $\zeta(\text{He}^+)$ be time-dependent.

As for the thermal heavy-ion contribution, it is negligible, since $E'_c \gg E'_0$ for all practical purposes.

III. COUPLED CHARGE-EXCHANGE AND ION-EMC EMISSION EFFECTS

To understand this Section, the reader will have to shift mental gears from Section II, where growth rates was calculated without considering the effect of wave emission on the distribution function f . The point is that f will become more anisotropic, thus increasing γ according to (2.12) only up to the time where $R \equiv 2\gamma\ell v_G^{-1}$ reaches unity. Let us call this time t_1 . After t_1 , finite-amplitude ion-EMC waves are emitted, and it is well-known that a necessary condition for wave-particle equilibrium is $R = 1$ for those frequencies at which finite-amplitude waves are present [Cornwall, 1966, 1975a; Kennel and Petschek, 1966]. (Note: $R = 1$ is only appropriate if there is no heavy-ion damping of the waves as they pass through the ring current. If the heavy-ion damping rate is $-\gamma_{He}$, $R = 1$ should be replaced by the larger value $R = 1 + 2\gamma_{He}\ell v_G^{-1}$. This qualification should be kept in mind whenever we discuss the condition $R = 1$.) For conditions appropriate to the December 17-18 storm, Figs. 2 and 3 and Eqs. (2.17) and (2.19) suggest that $\lambda_0 t_1$ can be as small as 0.2, which corresponds to fairly small values of the anisotropy (to be defined below).

The constancy of R in time for $t > t_1$ is achieved through a balance of the rates of change of the shape of the distribution function in y , of the cold plasma density, the decaying omnidirectional flux, etc. It is an enormously complicated job to evaluate the precise y -dependence of f which (a) keeps $R = 1$ over a finite frequency band width, (b) is consistent with particle losses from charge-exchange and pitch-angle scattering. (See Etcheto et al. [1973] for an attempt to solve a similarly complicated problem.) We try a much more modest program [Cornwall, 1975a], in which the shape of the distribution function is parametrized by just one number, the

anisotropy A . Now it is no longer possible to make $R = 1$ over a finite frequency bandwidth; instead we impose only the condition $\bar{R} = 1$, where \bar{R} is the value of R at the frequency \bar{x} which maximizes R . (The idea is that the fastest-growing waves largely determine the equilibrium between wave growth and loss.)

It is especially important to realize that A is a dynamical parameter, no longer given by a simple formula like (2.13). That is, A responds not only to charge-exchange growth (as in (2.13)) but also to loss of anisotropy by wave emission [Brice, 1964] and to increase of anisotropy from precipitation into the loss cone. Indeed, A must respond very rapidly by wave emission in order to keep \bar{R} at its equilibrium value of unity; no other parameter (e.g., E_0 , E_m , $\lambda_0 t$) can change at a rate comparable to the wave-growth time scale.

We have noted before [Cornwall, 1975a] that, of all the quantities on which \bar{R} depends, it depends most sensitively on A (at least if A is less than one). Thus the condition $\bar{R} = 1$ serves to determine A , primarily, and the constancy of \bar{R} suggests a similar near-constancy for A . As a first approximation, anisotropy growth from charge-exchange balances anisotropy loss from wave emission, and the shape of f evolves much more slowly during the period of wave emission than before. This approximation breaks down also at later times, when the flux has decayed so much that greater and greater anisotropy is needed to keep growth going.

We turn to the calculation of \bar{R} . The first problem is how to parametrize the shape of f by a single parameter A , in order to calculate \bar{R} . The actual shape is unknown, and such a parametrization will be useful only if similar results are achieved for a variety of (smooth) shape functions. For a shape given by a power law $f \sim y^{2A}$ or a bi-Maxwellian ($A = (T_{\perp}/T_{\parallel}) - 1$), numerous results are available in the literature. Numerical results for \bar{R}

are given in Cornwall [1975a] for the bi-Maxwellian case. In the present paper we consider instead distribution functions whose pitch-angle shape is given by (2.2), the charge-exchange form, except that $\lambda_0 t$ is replaced by a dynamical parameter τ equivalent to the anisotropy:

$$J(E,y,L) = J_0(L,t_1) e^\tau \exp\{-E/E_0 - \tau y^{-2}\}. \quad (3.1)$$

Of course, at the time t_1 when finite-amplitude wave emission begins, $\tau = \lambda_0 t_1$, but thereafter τ (or A) is determined by the condition $\bar{R} = 1$.

How is τ related to the anisotropy? For purposes of the quasi-linear moment equations, the anisotropy must be defined in terms of the expectation values $\langle NE \rangle$ and $\langle NE_\perp \rangle$ of the total energy and of the perpendicular energy. The expectation values would be correctly defined by

$$\langle Q \rangle = \int d\mu dJ fQ \sim \int dE dy y T(y) Q E^{1/2} f \quad (3.2)$$

for any function Q . The integrals are taken over the first two invariants μ, J at fixed L , and $T(y)$ is the normalized bounce time as defined by Schulz and Lanzerotti [1974]. Unfortunately the curvature of the field lines obscures to some extent some simple physical points we wish to make later on, so we define expectation values as simply integrals over the equatorial velocity components (as if the Earth's field lines were straight). Then the anisotropy A is defined as:

$$\langle NE_\perp \rangle = \langle NE \rangle \left(\frac{A+1}{A+\frac{3}{2}} \right). \quad (3.3)$$

The relation between τ and A is shown in Fig. 4; note that A grows at roughly twice the rate τ does. A comparison of A as defined by (3.2)

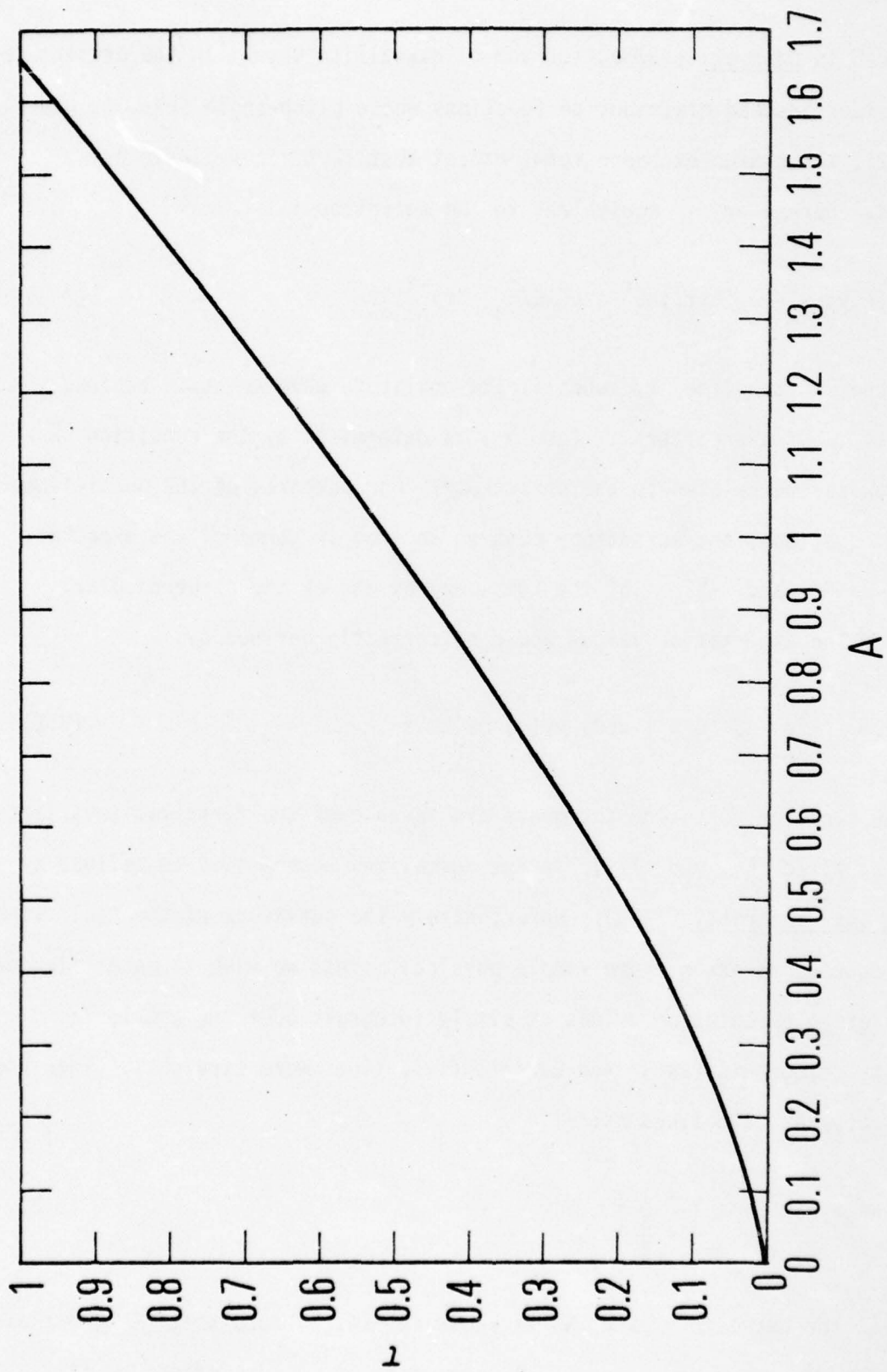


Figure 4. Pitch-angle shape parameter τ vs. anisotropy A .

with \bar{A}_{eff} (see (2.13)) shows discrepancies at the lowest values of A , but these are unimportant.

Given the distribution function (3.1), the calculation of \bar{R} (or equivalently the maximum growth rate) is the same as the calculations of Section II, except that $\lambda_0 t$ is replaced by τ , and except that f no longer decays in time in quite the same way as it would if only charge exchange were acting.

To explain this latter point, we observe that if A is roughly constant in time, protons must be scattered in pitch angle through a substantial fraction of 90° in one charge-exchange lifetime so that anisotropy loss from pitch-angle scattering can balance anisotropy growth from charge-exchange. In turn, this means that protons do not experience charge-exchange losses appropriate to a fixed pitch angle, but rather that all protons are lost by charge-exchange processes at a pitch-angle averaged rate Λ , defined by

$$\Lambda = \lambda_0 \frac{\langle y^{-2} \rangle}{\langle I \rangle} \quad (3.4)$$

Λ is, in fact, the loss rate which occurs in the quasi-linear moment-equation for $\langle N \rangle$ or $\langle NE \rangle$ as we discuss below. Fig. 5 shows a plot of $\Lambda \lambda_0^{-1}$ vs. A . Note that Λ is roughly twice λ_0 at small A , but at large A there are very few protons at small y , and here $\Lambda \approx \lambda_0$. In addition, protons are lost by precipitation into the loss cone due to pitch-angle scattering, and energy is lost by wave emission. These effects may be incorporated by allowing $J_0(L, t_1)$ and E_0 into (3.1) to be functions of time, whose time dependence is governed by the quasi-linear moment equations of the next Section as well as by the condition $\bar{R} = 1$.

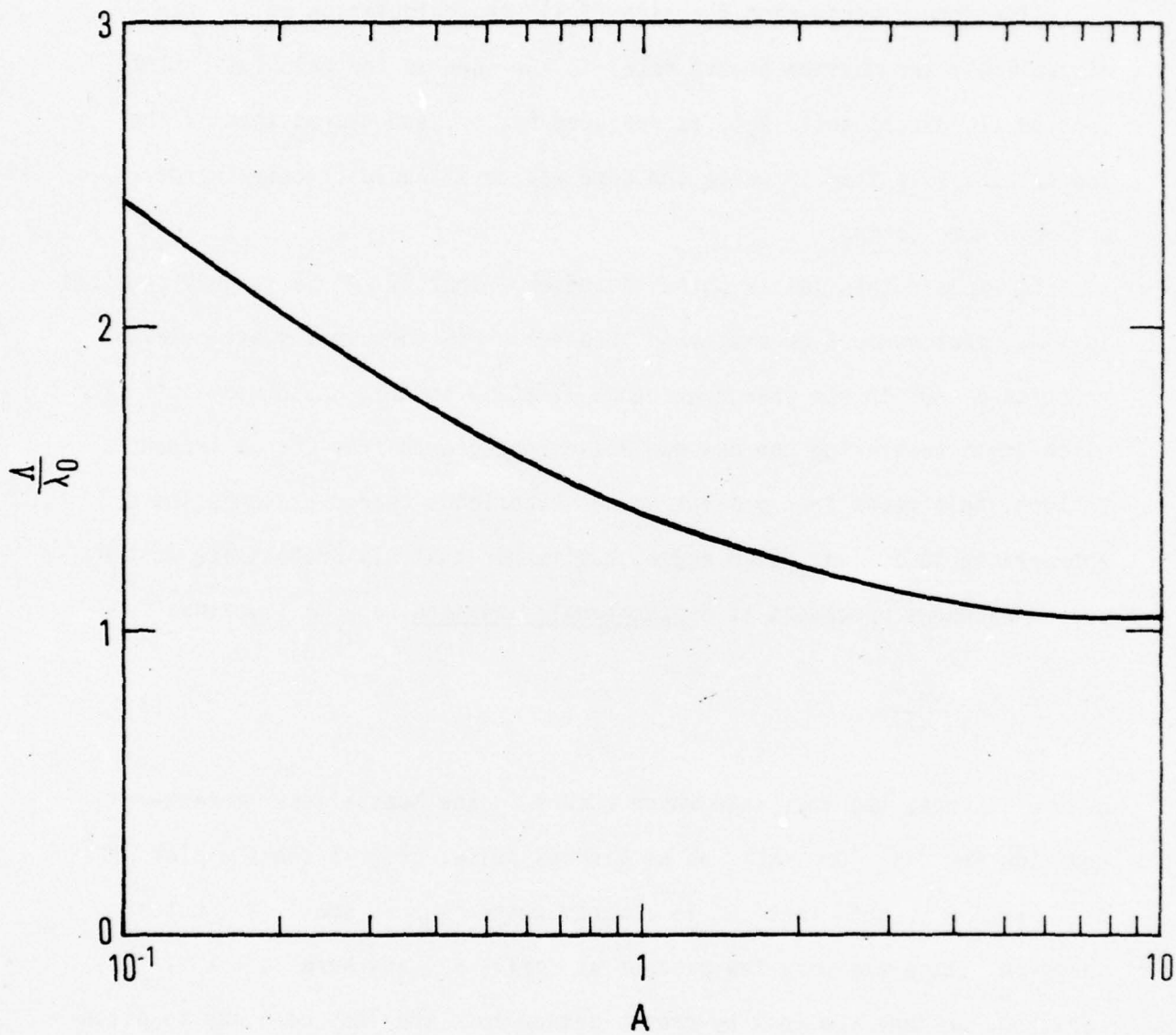


Figure 5. Pitch-angle averaged charge-exchange rate Λ vs. anisotropy A .

The upshot of all this discussion is the following formula for \bar{R} :

$$\bar{R} = 2\pi^2 J_0(L, t_1) \frac{M\Omega L}{N} \text{MAX}_x \left\{ \left(\frac{1-x}{x} \right) K_0(\tilde{z}) \left[\tau \left(\frac{1-x}{x} \right) - \frac{1}{1+\tilde{a}} \right] \exp[-E_c/E_0 - \Lambda(t-t_1)] \right\} \quad (3.5)$$

where $J_0(L, t_1)$ is the flux factor corresponding to the time t_1 at which wave emission starts (i.e., \bar{R} first attains the value of unity). In (3.5), \tilde{z} and \tilde{a} are calculated as in (2.8), with τ substituted for $\lambda_0 t$ (except in E_c). As a function of A , \bar{R} shows the same features as it would for a bi-Maxwellian: a steep dependence on A for $A < 1$. This is illustrated in Fig. 6, where the A -dependence of \bar{R} is isolated in the expression

$$\Gamma_{\text{MAX}} = \bar{R} e^{\Lambda(t-t_1)} \left[2\pi^2 J_0(L, t_1) \frac{M\Omega L}{N} \right]^{-1} \quad (3.6)$$

for $E_m/E_0 \approx 0.21$. The interested reader should compare Fig. 6 to Fig. 1 of Cornwall [1975a] which gives \bar{R} for a bi-Maxwellian; the A -dependence of \bar{R} is quite similar for the two cases.

In the next Section, we use $\bar{R} = 1$ as a dynamic equation relating the parameters which appear in (3.5). This equation is adjoined to the quasi-linear equations for the distribution function, yielding a set of equations from which the emitted wave energy can be calculated, as well as the evolution of A , $\langle N \rangle$, and $\langle NE \rangle$.

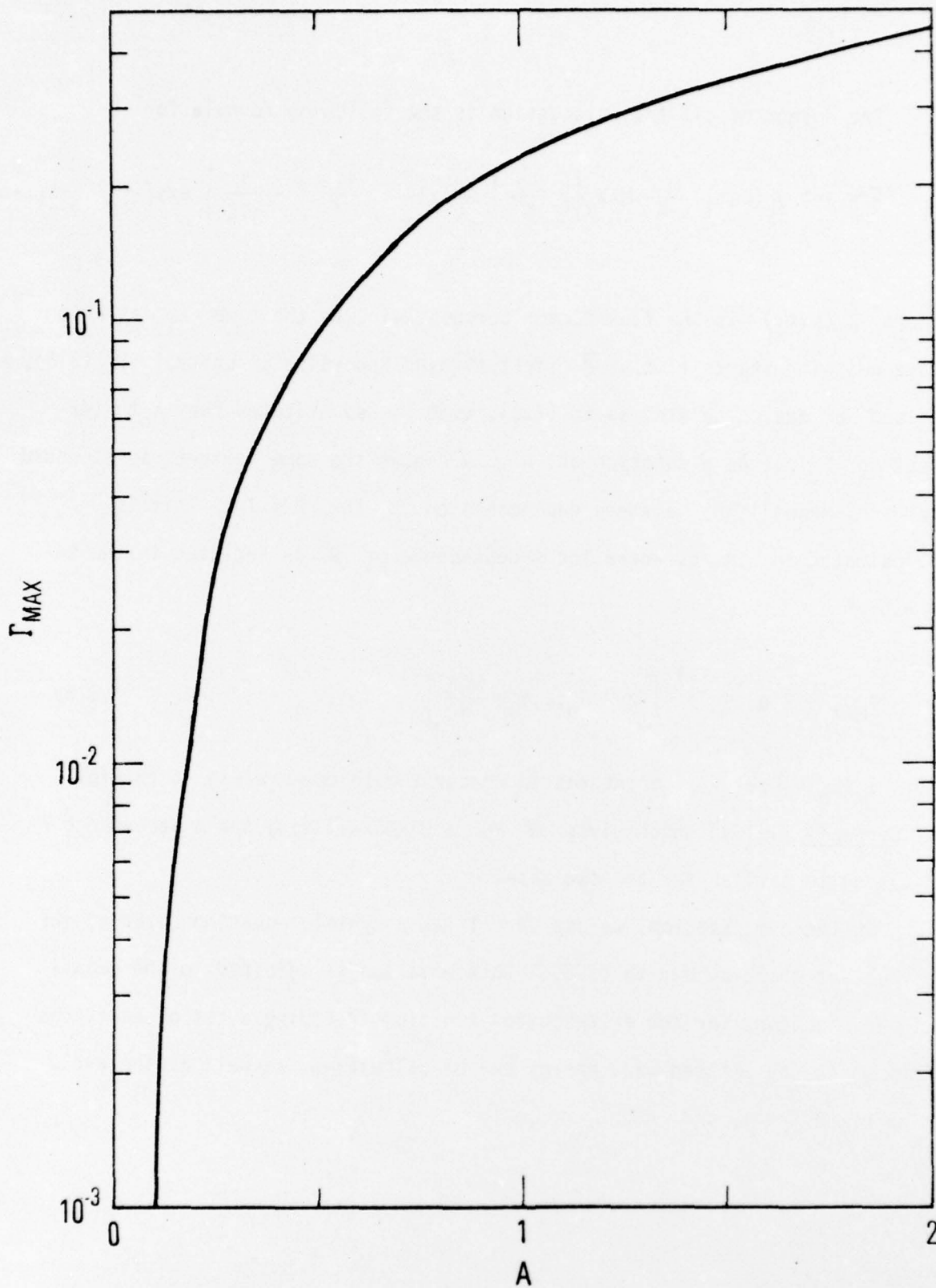


Figure 6. Dependence of the maximum growth rate Γ_{MAX} on anisotropy A . To normalize, see Eq. (3.6).

IV. DYNAMICS ACCORDING TO THE MOMENT TRANSPORT EQUATIONS

In addition to the equation for $\bar{R} = 1$ discussed in the last Section, there is the quasi-linear diffusion equation expressing the rate of change of f as determined by charge exchange, loss-cone precipitation, and wave-induced diffusion. We replace this equation by a set of moment equations [Cornwall, 1975a] for the moments $\langle N \rangle$, $\langle NE \rangle$, and $\langle NE_{\perp} \rangle$. Actually we need only consider equations for $\langle NE \rangle$ and $\langle NE_{\perp} \rangle$, since $\langle N \rangle$ does not appear in these two moment equations.

The main objectives of this Section are to determine the rate at which particle energy is lost to waves, and to discuss the evolution of the anisotropy during the period of wave emission. It will be very helpful to consider a simplified version of the energy-loss problem, following Brice [1964]. He points out that the conservation of energy and momentum during the elementary process of emission of a wave quantum by a single particle lends to a relation between the rate \dot{E}_W at which the particle loses energy to waves and the rate $\dot{E}_{\perp W}$ at which it loses perpendicular energy:

$$\dot{E}_W / \dot{E}_{\perp W} = \omega / \Omega \quad (4.1)$$

Assume that $E/E_{\perp} \approx \langle NE \rangle / \langle NE_{\perp} \rangle$; then with the aid of the definition (3.3) of the anisotropy A , we find

$$A = \frac{\frac{3}{2} E_{\perp} - E}{E - E_{\perp}} \quad (4.2)$$

It is simple to combine (4.1) and the time derivative of (4.2) to find

$$\frac{\dot{E}_W}{E} = \frac{x \dot{A}_W}{2 \left(A + \frac{3}{2} \right)^2} \left[1 - x \frac{(A+1)}{\left(A + \frac{3}{2} \right)} \right]^{-1} \quad (4.3)$$

where $x = \omega/\Omega$. Here \dot{A}_W is the rate at which anisotropy is lost by wave emission. Note that, since the emission frequency is bounded by $x < A(1+A)^{-1}$, the square brackets in (4.3) are always positive. If (as argued in the last Section) A is roughly constant, then $-\dot{A}_W$ must roughly be equal to \dot{A}_{CEX} , the rate at which A increases by charge exchange. For a distribution function of the type (3.1), we have

$$\dot{A}_{\text{CEX}} = \frac{dA}{d\tau} \dot{\tau} = \lambda_0 \frac{dA}{d\tau} \approx 2\lambda_0 \quad (4.4)$$

where we consulted Fig. 4 for $dA/d\tau$. Thus (4.3) yields \dot{E}_W/E in terms of λ_0 , A , and x . For typical values of A and x , \dot{E}_W/E is 15-20% of λ_0 ; in words, the particles lose energy to waves at ~15% of the rate at which they lose energy by charge exchange. We shall see below that this rate is somewhat larger when (4.3) is modified to account for precipitation losses, but even this rate is enough to power SAR-arcs. For example, during recovery phase of the December 17-18 storm, the total energy stored in the ring current is of the order 5×10^3 ergs cm^{-2} (energy per unit area at the ionosphere), and it is dissipated at a rate of ≈ 0.3 ergs $\text{cm}^{-2} \text{sec}^{-1}$ by charge exchange. Twenty percent of this is 0.06 ergs $\text{cm}^{-2} \text{sec}^{-1}$, while it is estimated by Williams et al. [1976] that roughly 0.05 ergs $\text{cm}^{-2} \text{sec}^{-1}$ is needed to power the observed SAR-arcs during this storm. The SAR arc begins to fade rapidly about 10 hours (or $2\lambda_0^{-1}$) into recovery phase.

Eq. (4.3) does not take into account a number of effects; to remedy this, we turn to the moment-transport equations. We refer the reader to Cornwall [1975a] for all details. The equation for $\langle NE_1 \rangle$ reads

$$\frac{\partial}{\partial t} \langle NE_1 \rangle = -\langle \lambda NE_1 \rangle - 2\bar{\gamma} \bar{W} x^{-1}. \quad (4.5)$$

\bar{W} is essentially the energy density of the waves. Note that there is no precipitation loss term, since the equatorial value of E is very small in the loss cone.

The first step is to express all the terms in (4.5) in terms of A and $\langle NE \rangle$. Since $\lambda = \lambda_0 y^{-2}$, $E = Ey^2$, $\langle \lambda NE \rangle = \lambda_0 \langle NE \rangle$. The process is completed by using the definition (3.3) of A , and we express the result as an equation for $2\bar{\gamma} \bar{W}$:

$$2\bar{\gamma} \bar{W} = x \left\{ -\lambda_0 \langle NE \rangle - \left(\frac{A+1}{A+\frac{3}{2}} \right) \frac{\partial}{\partial t} \langle NE \rangle - \frac{-\dot{A}}{2 \left(A + \frac{3}{2} \right)^2} \langle NE \rangle \right\}. \quad (4.6)$$

The idea is to combine (4.6) with the moment equation for $\langle NE \rangle$, eliminate $\partial/\partial t \langle NE \rangle$, and thus arrive at an equation for $2\bar{\gamma} \bar{W}$ which contains no time derivatives. The $\langle NE \rangle$ moment equation is

$$\frac{\partial}{\partial t} \langle NE \rangle = -\Lambda \langle NE \rangle - 2\bar{\gamma} \bar{W} - \langle \lambda_p NE \rangle \quad (4.7)$$

where we have used (3.4) to write $\langle \lambda NE \rangle = \Lambda \langle NE \rangle$. The last term in (4.7) represents precipitation into the loss cone produced by wave diffusion. By eliminating $2\bar{\gamma} \bar{W}$ from (4.7) we find

$$\frac{\partial}{\partial t} \langle NE \rangle = d^{-1} \left\{ -(\Lambda - x\lambda_0) \langle NE \rangle + \frac{\dot{A}}{\left(A + \frac{3}{2} \right)^2} \langle NE \rangle - \langle \lambda_p NE \rangle \right\} \quad (4.8)$$

where

$$d = 1 - x \left(\frac{A+1}{A+\frac{3}{2}} \right) > \left(\frac{2}{3} A + 1 \right)^{-1}. \quad (4.9)$$

The inequality follows from $x < A/(A+1)$. Alternatively we eliminate $\partial/\partial t \langle NE \rangle$ from (4.6) to find

$$2\bar{\gamma} \bar{W} = d^{-1} x \left\{ \left[\Lambda \frac{(A+1)}{A + \frac{3}{2}} - \lambda_0 \right] \langle NE \rangle + \left(\frac{A+1}{A + \frac{3}{2}} \right) \langle \lambda_p NE \rangle - \frac{\dot{A} \langle NE \rangle}{2 \left(A + \frac{3}{2} \right)^2} \right\}. \quad (4.10)$$

The analog of $-\dot{E}_W E^{-1}$ in the simplified Brice model (4.3) is $2\bar{\gamma} \bar{W} \langle NE \rangle^{-1}$. It is easily checked that, if the charge-exchange and precipitation loss terms in (4.10) are dropped, (4.10) reduces to (4.3) (with, of course, $\dot{A} = \dot{A}_W$). Furthermore, the term in square brackets in (4.10) represents the growth of anisotropy from charge exchange. To see this, substitute $\partial/\partial t \langle NE_1 \rangle = -\lambda_0 \langle NE \rangle$ and $\partial/\partial t \langle NE \rangle = -\Lambda \langle NE \rangle$ in the time derivative of the definition (3.3) of A , and come to

$$\frac{\dot{A}_{CEX}}{2 \left(A + \frac{3}{2} \right)^2} = \Lambda \left(\frac{A+1}{A + \frac{3}{2}} \right) - \lambda_0 \quad (4.11)$$

which, in turn, is easily shown to be identical to (4.4) with the help of (3.1), (3.3), and (3.4). Since $\dot{A} = \dot{A}_{CEX} + \dot{A}_W$, (4.10) can be written

$$2\bar{\gamma} \bar{W} = d^{-1} x \left\{ - \frac{\dot{A}_W \langle NE \rangle}{2 \left(A + \frac{3}{2} \right)^2} + \left(\frac{A+1}{A + \frac{3}{2}} \right) \langle \lambda_p NE \rangle \right\} \quad (4.12)$$

which is again the simple Brice relation (4.3) except for the $\langle \lambda_p NE \rangle$ term.

It only remains to discuss $\langle \lambda_p NE \rangle$, the precipitation-loss term coming from pitch-angle scattering. We have already argued that a particle changes its pitch angle at about the charge-exchange rate, so we expect

$\langle \lambda_p NE \rangle \sim \lambda_0 \langle NE \rangle$ or possibly $\Lambda \langle NE \rangle$. This means that the waves are in the weak-diffusion regime, because the characteristic pitch-angle diffusion time λ_0^{-1} is considerably smaller than the average minimum lifetime $\bar{T}_{MIN} \approx T_B / 2\alpha_0^2$ where T_B is the bounce time and α_0 the loss-cone pitch angle. However, it is possible that there is a transient regime in which strong diffusion occurs, if $\langle NE \rangle$ at the time t_1 (when the waves switch on) is quite large compared to a critical value (discussed in Cornwall [1975a]) which is roughly comparable to the stably-trapped limit of Kennel and Petschek [1966]. This transient regime ends when strong diffusion has reduced $\langle NE \rangle$ to a value comparable to the critical value $\langle NE \rangle_c$.

In order to discuss both the strong-diffusion transient and the weak-diffusion regime together, it is necessary to take into account the non-linear dependence of $\langle \lambda_p NE \rangle$ on $2\bar{\gamma} \bar{W}$. In an earlier work [Cornwall, 1975a] we introduced the form

$$\langle \lambda_p NE \rangle = 2\bar{\gamma} \bar{W} \langle NE \rangle \left[\langle NE \rangle_c \frac{(A+1)x}{d \left(A + \frac{3}{2} \right)} + \bar{T}_{MIN} 2\bar{\gamma} \bar{W} \right]^{-1}. \quad (4.13)$$

The term linear in \bar{W} (found by setting $\bar{T}_{MIN} = 0$) yields the weak-diffusion limit, while in the strong-diffusion limit $\langle \lambda_p NE \rangle \rightarrow \langle NE \rangle \bar{T}_{MIN}^{-1}$. The critical value $\langle NE \rangle_c$ is approximately

$$\langle NE \rangle_c \approx \frac{B^2}{4\pi} \left(\frac{\bar{v}_p}{\ell \bar{\omega}} \right) \frac{d \left(A + \frac{3}{2} \right)}{(A+1)}. \quad (4.14)$$

Use (4.13) in (4.10) to find

$$2\bar{\gamma} \bar{W} = \frac{x}{2d\bar{T}_{MIN}} \left(\frac{A+1}{A+\frac{3}{2}} \right) \left[Q + (Q^2 + 4\bar{T}_{MIN} Y \langle NE \rangle_c)^{1/2} \right] \quad (4.15)$$

where

$$Q = \langle NE \rangle - \langle NE \rangle_c + \bar{T}_{MIN} \gamma \quad (4.16)$$

$$\gamma = \left[\Lambda - \left(\frac{A + \frac{3}{2}}{A + 1} \right) \lambda_0 \right] \langle NE \rangle - \frac{\dot{A} \langle NE \rangle}{2(A+1) \left(A + \frac{3}{2} \right)}. \quad (4.17)$$

From (4.15) various limits can be found. When $\bar{T}_{MIN} \gamma \gg |\langle NE \rangle - \langle NE \rangle_c|$, we find that $2\bar{\gamma} \bar{W}$ is given by the right-hand side of (4.10), with $\langle \lambda_p NE \rangle$ set equal to zero. When $\langle NE \rangle - \langle NE \rangle_c \gg \bar{T}_{MIN} \gamma$, we find

$$2\bar{\gamma} \bar{W} = \frac{x}{d\bar{T}_{MIN}} \left(\frac{A + 1}{A + \frac{3}{2}} \right) \left[\langle NE \rangle - \langle NE \rangle_c \right]. \quad (4.18)$$

This is the limit which was studied earlier [Cornwall, 1975a]. It amounts to saying that precipitation losses are much more important than charge-exchange losses, which is true for several special cases. The first case is that of electron EMC waves generated by energetic electrons, for which there is no charge exchange. The second case is the transient regime mentioned above for the proton ring current, when the waves switch on in a very strong ring current. The waves grow rapidly, and precipitation losses reduce $\langle NE \rangle - \langle NE \rangle_c$ to order of $\bar{T}_{MIN} \gamma$, at which time all quantities begin to change more or less on the charge-exchange time scale.

We may estimate the size of $2\bar{\gamma} \bar{W}$ in the weak-diffusion regime by supposing $\langle NE \rangle - \langle NE \rangle_c \approx \bar{T}_{MIN} \gamma$. There is, under these circumstances, a term in (4.15) of order $\lambda_0 (\lambda_0 \bar{T}_{MIN})^{-1/2} \langle NE \rangle$, plus terms of $O(\lambda_0 \langle NE \rangle)$. Since a typical value of $(\lambda_0 \bar{T}_{MIN})^{-1}$ is about 5, this square-root term is not an order of magnitude greater than the terms of $O(\lambda_0)$, and the whole of (4.15) is, practically speaking, $O(\lambda_0 \langle NE \rangle)$. In other words, the precipitation

loss term $\langle \lambda_p \text{NE} \rangle$ in (4.12) is of order $\lambda_0 \langle \text{NE} \rangle$, as would be expected if the pitch-angle diffusion coefficient is $O(\lambda_0)$.

As time goes on, another sort of weak-diffusion regime sets in. In this regime, it is no longer true that \dot{A} is small and that $Y \approx O(\lambda_0 \langle \text{NE} \rangle)$. Rather, $Y \approx O(\bar{T}_{\text{MIN}} \lambda_0^2 \langle \text{NE} \rangle)$, which means that the anisotropy is growing at very nearly the charge exchange rate (cf. (4.17) and (4.11)). Also, $|\langle \text{NE} \rangle - \langle \text{NE} \rangle_c| \approx O(\lambda_0 \bar{T}_{\text{MIN}} \langle \text{NE} \rangle_c)$, and $2\bar{Y} \bar{W} \approx O(\lambda_0 \langle \text{NE} \rangle)$. Ultimately, as the flux decays, this ordering of $\langle \text{NE} \rangle - \langle \text{NE} \rangle_c$ will be violated and one finds $2\bar{Y} \bar{W} \approx \lambda_0^2 \bar{T}_{\text{MIN}} \langle \text{NE} \rangle$. At this point wave emission has effectively ceased, if it has not already been forced to cease because it is no longer possible to satisfy $\bar{R} = 1$.

The quantitative statement of these effects requires simultaneous solution of the equation $\bar{R} = 1$ (see Eq. (3.5)) and the $\partial \langle \text{NE} \rangle / \partial t$ Eq. (4.7) which can be written, using (4.13) and (4.15), as

$$\frac{\partial}{\partial t} \langle \text{NE} \rangle = -\Lambda \langle \text{NE} \rangle - \frac{Z}{\bar{T}_{\text{MIN}}} \left[\frac{x(A+1)}{2d \left[A + \frac{3}{2} \right]} + \frac{\langle \text{NE} \rangle}{2 \langle \text{NE} \rangle_c + Z} \right] \quad (4.19)$$

$$Z = Q + (Q^2 + 4\bar{T}_{\text{MIN}} Y \langle \text{NE} \rangle_c)^{1/2}. \quad (4.20)$$

Although some preliminary efforts have been made in this direction, they do not add appreciably to our qualitative understanding as described earlier. This understanding may be summarized as follows:

There are three terms in $2\bar{Y} \bar{W}$ as given in (4.10). The first (in square brackets) corresponds to the growth of anisotropy from charge exchange. The second (precipitation-loss) term is estimated to be $\approx \lambda_0 \langle \text{NE} \rangle$. The third term involving $-\dot{A}$ is smaller than the other two terms until wave growth is about to end, when it nearly cancels the first term (i.e., Y in

(4.17) becomes small). During the main wave-growth period when $\dot{A} \approx 0$, the precipitation-loss term may add significantly to $2\bar{\gamma}\bar{W}$, perhaps even doubling the result coming from charge exchange alone. That is, the naive Brice relation (4.3) may only yield one-half the energy lost to waves, which could thus be 20-40% of the energy lost by charge exchange. In view of the imperfectly efficient processes by which wave energy is used to heat electrons, this should be approximately right to drive SAR-arcs.

APPENDIX

The mathematical task is to evaluate Eq. (8), for constant λ_0 . The relevant integral is

$$I = \int_{E_c}^{\infty} \frac{dE}{E} \left[-1 + \left(\frac{1-x}{x} \right) \frac{\lambda_0 t E}{E-E_c} \right] \exp \left\{ -\frac{E}{E_0} - \frac{\lambda_0 t E_c}{E-E_c} \right\}. \quad (\text{A.1})$$

The change of variables

$$q = \frac{2}{zE_0} (E-E_c) \quad (\text{A.2})$$

yields

$$I = e^{-E_c/E_0} \int_0^{\infty} dq \left[-\frac{1}{q+a} + \left(\frac{1-x}{x} \right) \frac{\lambda_0 t}{q} \right] \exp \left\{ -\frac{z}{2} \left(q + \frac{1}{q} \right) \right\}. \quad (\text{A.3})$$

With the aid of a standard formula for Hankel functions of imaginary argument

$$K_\nu(bz) = \frac{1}{2} b^\nu \int_0^{\infty} dt t^{\pm\nu-1} \exp \left\{ -\frac{z}{2} \left(t + \frac{b^2}{t} \right) \right\} \quad (\text{A.4})$$

we find

$$I = e^{-E_c/E_0} \left[2 \left(\frac{1-x}{x} \right) \lambda_0 t K_0(z) - Q(a, z) \right] \quad (\text{A.5})$$

where

$$Q(a, z) = \int_0^{\infty} \frac{dq}{q+a} \exp \left\{ -\frac{z}{2} \left(q + \frac{1}{q} \right) \right\}. \quad (\text{A.6})$$

Evidently $Q(0,z) = 2K_0(z)$, from (A.4), and Q is a positive decreasing function of a for positive a . In (A.6), the change of variables $q \rightarrow q^{-1}$ easily yields, along with (A.4),

$$Q(a,z) + Q(a^{-1}, z) = 2K_0(z) \quad (\text{A.7})$$

from which $Q(1,z) = K_0(z)$. One may give a formal expansion of (A.6) as a power series in a (or in a^{-1}), with coefficients $K_N(z)$, but this is not very useful. By writing the denominator of (A.6) in the form

$$\frac{1}{q+a} = \int_0^{\infty} d\lambda e^{-\lambda(q+a)} \quad (\text{A.8})$$

some useful forms can be derived. We quote only one of them:

$$Q(a,z) = 2K_0(z) - e^{\frac{1}{2}az} \int_{az}^{\infty} d\lambda e^{-\frac{1}{2}\lambda} K_0\left[\left[\frac{z\lambda}{a}\right]^{1/2}\right]. \quad (\text{A.9})$$

Finally, a very simple and useful approximation follows from the steepest-descent evaluation of (A.6) for large z . It is:

$$Q(a,z) \approx \frac{2K_0(z)}{1+a}. \quad (\text{A.10})$$

This satisfies (A.7) for all z . The approximation (A.10) is an overestimate of Q for $0 < a < 1$. It is useful even for small z ; the maximum error is about 15% for $z = 0.1$.

REFERENCES

- Brice, N., Fundamentals of Very Low Frequency Emission Generation Mechanisms, J. Geophys. Res. 69, 4515, 1964.
- Cornwall, J. M., Micropulsations and the Outer Radiation Zone, J. Geophys. Res. 71, 2185, 1966.
- Cornwall, J. M., Moment Transport Equations for Wave-Particle Interactions in the Magnetosphere, J. Geophys. Res. 80, 4635, 1975a.
- Cornwall, J. M., Density-Sensitive Instabilities in the Magnetosphere, invited talk at the IUGG General Assembly, Grenoble, France, August 1975b.
- Cornwall, J. M., F. V. Coroniti, and R. M. Thorne, Turbulent Loss of Ring Current Protons, J. Geophys. Res. 75, 4699, 1970.
- Cornwall, J. M., F. V. Coroniti, and R. M. Thorne, A Unified Theory of SAR Arc Formation at the Plasmapause, J. Geophys. Res. 76, 4428, 1971.
- Cornwall, J. M., A. R. Sims, and R. S. White, Atmospheric Density Experienced by Radiation Belt Protons, J. Geophys. Res. 70, 3099, 1965.
- Etcheto, J., R. Gendrin, J. Solomon, and A. Roux, A Self-Consistent Theory of Magnetospheric Hiss, J. Geophys. Res. 78, 8150, 1973.
- Joselyn, J. A., and L. R. Lyons, Ion Cyclotron Wave Growth Calculated from Satellite Observations of the Proton Ring Current During Storm Recovery, J. Geophys. Res. 81, 2275, 1976.
- Kennel, C. F., and H. E. Petschek, Limit on Stably Trapped Particle Fluxes, J. Geophys. Res. 71, 1, 1966.
- Liemohn, H., The Lifetime of Radiation Belt Protons with Energies between 1 keV and 1 MeV, J. Geophys. Res. 66, 3593, 1961.
- Lyons, L. R., and D. S. Evans, The Inconsistency between Proton Charge Exchange and the Observed Ring Current Decay, submitted to J. Geophys. Res., 1976.

- Schulz, J., and L. Lanzerotti, Particle Diffusion in the Radiation Belts, Springer-Verlag, Berlin, 1974.
- Shelley, E. G., R. G. Johnson, and R. D. Sharp, Morphology of Energetic O^+ in the Magnetosphere, in Magnetospheric Physics, ed. B. M. McCormac, p. 135, D. Reidel, Dordrecht, Netherlands, 1974.
- Smith, P. H., R. A. Hoffmann, and T. Fritz, Ring Current Proton Decay by Charge Exchange, J. Geophys. Res. 81, 2701, 1976.
- Swisher, R. L., and L. A. Frank, Lifetimes for Low-Energy Protons in the Outer Radiation Zone, J. Geophys. Res. 73, 5665, 1968.
- Tinsley, Brian A., Evidence that the Recovery Phase Ring Current Consists of Helium Ions, submitted to J. Geophys. Res., 1976.
- Williams, D. J., and L. R. Lyons, The Proton Ring Current and its Interaction with the Plasmopause: Storm Recovery Phase, J. Geophys. Res. 79, 4195, 1974a.
- Williams, D. J., and L. R. Lyons, Further Aspects of the Proton Ring Current Interaction with the Plasmopause: Main and Recovery Phases, J. Geophys. Res. 79, 4791, 1974b.
- Williams, D. J., G. Hernandez, and L. R. Lyons, Simultaneous Observations of the Proton Ring Current and Stable Auroral Red Arcs, J. Geophys. Res. 81, 608, 1976.

LABORATORY OPERATIONS

The Laboratory Operations of The Aerospace Corporation is conducting experimental and theoretical investigations necessary for the evaluation and application of scientific advances to new military concepts and systems. Versatility and flexibility have been developed to a high degree by the laboratory personnel in dealing with the many problems encountered in the nation's rapidly developing space and missile systems. Expertise in the latest scientific developments is vital to the accomplishment of tasks related to these problems. The laboratories that contribute to this research are:

Aerophysics Laboratory: Launch and reentry aerodynamics, heat transfer, reentry physics, chemical kinetics, structural mechanics, flight dynamics, atmospheric pollution, and high-power gas lasers.

Chemistry and Physics Laboratory: Atmospheric reactions and atmospheric optics, chemical reactions in polluted atmospheres, chemical reactions of excited species in rocket plumes, chemical thermodynamics, plasma and laser-induced reactions, laser chemistry, propulsion chemistry, space vacuum and radiation effects on materials, lubrication and surface phenomena, photo-sensitive materials and sensors, high precision laser ranging, and the application of physics and chemistry to problems of law enforcement and biomedicine.

Electronics Research Laboratory: Electromagnetic theory, devices, and propagation phenomena, including plasma electromagnetics; quantum electronics, lasers, and electro-optics; communication sciences, applied electronics, semiconducting, superconducting, and crystal device physics, optical and acoustical imaging; atmospheric pollution; millimeter wave and far-infrared technology.

Materials Sciences Laboratory: Development of new materials; metal matrix composites and new forms of carbon; test and evaluation of graphite and ceramics in reentry; spacecraft materials and electronic components in nuclear weapons environment; application of fracture mechanics to stress corrosion and fatigue-induced fractures in structural metals.

Space Sciences Laboratory: Atmospheric and ionospheric physics, radiation from the atmosphere, density and composition of the atmosphere, aurorae and airglow; magnetospheric physics, cosmic rays, generation and propagation of plasma waves in the magnetosphere; solar physics, studies of solar magnetic fields; space astronomy, x-ray astronomy; the effects of nuclear explosions, magnetic storms, and solar activity on the earth's atmosphere, ionosphere, and magnetosphere; the effects of optical, electromagnetic, and particulate radiations in space on space systems.

THE AEROSPACE CORPORATION
El Segundo, California